Magnetic Resonance Imaging Detection of Intraplaque Hemorrhage

Magnetic Resonance Insights
Volume 10: 1–8

DOI: 10.1177/1178623X17694150

J Scott McNally[1], Seong-Eun Kim[1], Jason Mendes[1], J Rock Hadley[1], Akihiko Sakata[1], Adam H De Havenon[2], Gerald S Treiman[1] and Dennis L Parker[1]

[1]Utah Center for Advanced Imaging Research, Department of Radiology and Imaging Sciences, The University of Utah, Salt Lake City, UT, USA. [2]Department of Neurology, The University of Utah, Salt Lake City, UT, USA.

ABSTRACT: Carotid artery atherosclerosis is a major cause of ischemic stroke. For more than 30 years, future stroke risk and carotid stroke etiology have been determined using percent diameter stenosis based on clinical trials in the 1990s. In the past 10 years, magnetic resonance imaging (MRI) sequences have been developed to detect carotid intraplaque hemorrhage. By detecting carotid intraplaque hemorrhage, MRI identifies potential stroke sources that are often overlooked by lumen imaging. In addition, MRI can dramatically improve assessment of future stroke risk beyond lumen stenosis alone. In this review, we discuss the use of heavily T1-weighted MRI sequences used to detect carotid intraplaque hemorrhage. In addition, advances in ciné imaging, motion robust techniques, and specialized neck coils will be reviewed. Finally, the clinical use and future impact of MRI plaque hemorrhage imaging will be discussed.

KEYWORDS: MRI, intraplaque hemorrhage, atherosclerosis, stroke

RECEIVED: October 29, 2016. **ACCEPTED:** January 25, 2017.

PEER REVIEW: Three peer reviewers contributed to the peer review report. Reviewers' reports totaled 265 words, excluding any confidential comments to the academic editor.

TYPE: Review

FUNDING: The author(s) disclosed receipt of the following financial support for the research, authorship, and/or publication of this article: This study is supported by RSNA Research & Education Foundation Research Scholar Grant (Principal Investigator [PI] McNally), University of Utah Vice President for Research Intramural Seed Grant (PI McNally), Veterans Affairs Merit Review Award (PI Treiman), and NIH R01 Grant HL127582 (PI Parker).

DECLARATION OF CONFLICTING INTERESTS: The author(s) declared no potential conflicts of interest with respect to the research, authorship, and/or publication of this article.

CORRESPONDING AUTHOR: J Scott McNally, Utah Center for Advanced Imaging Research, Department of Radiology and Imaging Sciences, The University of Utah, 30 North 1900 East #1A071, Salt Lake City, UT 84132-2140, USA.
Email: scott.mcnally@hsc.utah.edu

Introduction

Cardiovascular disease and stroke are among the leading causes of morbidity and mortality in the United States, with total yearly costs exceeding $300 billion.[1] Large artery (eg, carotid) atherosclerosis is the cause of approximately 200 000 or 25% of the 795 000 ischemic strokes occurring each year.[2] Historically, carotid stenosis severity has been used to stratify patients to surgery or medical treatment. In 1991, the North American Symptomatic Carotid Endarterectomy Trial (NASCET) cemented the role of carotid stenosis as a predictor of stroke risk, leading to our current approach for intervention.[3] In symptomatic patients with ⩾70% stenosis, NASCET found that surgery outperformed medical therapy with a number needed to treat (NNT) of 6. Soon after NASCET, the Asymptomatic Carotid Artery Stenosis (ACAS) trial found surgery to be beneficial in asymptomatic patients with ⩾60% stenosis with a higher NNT of 19.[4]

Although the importance of carotid atherosclerosis as a cause of ischemic stroke cannot be disputed, percent stenosis is an imperfect predictor of future stroke risk. Despite the proven benefit of operative treatment, most patients with carotid disease will not have a subsequent stroke. If stenotic but stable plaques could be identified, many surgeries and health care expenses could be eliminated. Cerebral ischemic events related to carotid plaque are associated with plaque instability, but not necessarily hemodynamic compromise from stenosis, which does not reduce blood flow until it exceeds 90% narrowing.[5–21] The American Heart Association (AHA) has been working toward the goal of improving cardiovascular health by reducing death from cardiovascular diseases and stroke.[22] Recent advances in carotid plaque magnetic resonance imaging (MRI) may help achieve this goal by better diagnosing unstable carotid plaque by detection of vulnerable plaque components, including intraplaque hemorrhage (IPH).

Clinical Importance of Carotid IPH

Atherosclerosis causes morbidity and mortality largely due to AHA type IV (atheroma) and type V (fibroatheroma) lesions, in which there is disruption of the plaque surface, thrombus formation, and potential embolism.[23] If these plaques have superimposed IPH, this indicates an AHA type VIb or "complicated" plaque. Type VI plaques are often associated with symptoms and severely stenotic (obstructive) lesions. Still, type VI plaques can occur even without stenosis. In fact, most of the coronary events are associated with <50% stenosis.[24] Large clinical trials have found that the benefit of carotid endarterectomy is blunted in the setting of severe stenosis or near occlusion, and it is postulated that the potential for thromboembolism is greatly reduced when the distal artery is severely narrowed.[25–27] These findings suggest that thromboembolic potential is primarily linked to plaque characteristics, and flow

limitation may only determine the extent of infarction and may not be the primary cause.

Intraplaque hemorrhage is thought to result from plaque microvessel leakage during bouts of hypertension, leading to plaque progression and instability.[28–32] Intraplaque hemorrhage increases the necrotic core size and plaque volume, both of which are markers of plaque instability.[18] Prospective studies have found that carotid IPH leads to continued plaque growth and stenosis progression.[33] Microhemorrhages in the necrotic core lead to a feed-forward mechanism of further plaque growth and instability.[7] Thin, ruptured fibrous cap or plaque fissure, another culprit of vulnerable plaque progression, is highly associated with IPH.[34–36] Despite these plausible mechanisms of IPH, and our ability to detect it, no treatment has been shown to reverse these lesions, and no randomized trials have been conducted.

Multiple retrospective studies evaluating plaque composition have been performed, and subgroup analyses have found that IPH is important in stroke risk stratification.[5,19,37–41] Of carotid plaque components, IPH is of particular interest both because it increases future risk of ischemic stroke[7,9,12,13,15–18,28,41–46] and it occurs in approximately one-third of asymptomatic and a higher proportion of symptomatic carotid lesions with at least 50% stenosis.[10,11,18] Heterogeneous plaques with IPH have been correlated with a higher incidence of prior embolic stroke[9,16,17,40,45] and white matter lesions.[14] Early meta-analyses of 8 longitudinal studies found that the presence of IPH was associated with a ~6-fold increased risk of ischemic events (hazard ratio [HR]: 5.7) with higher risk in symptomatic (HR: 11.7) than asymptomatic (HR: 3.5) subjects.[16,18,47] Three recent meta-analyses from 2013 also demonstrated that a high percentage of patients with symptomatic IPH will have repeat stroke, with annual risk ranging from 15% to 45%.[48–50] This is despite standard medical therapy, including 3-hydroxy-3-methylglutaryl-coenzyme A reductase inhibitors (statins), antiplatelet medication, and blood pressure control. Recent and ongoing studies indicate that IPH signifies a high risk of stroke, independent of carotid stenosis, and is an important marker of carotid plaque vulnerability.[51,52] Computer simulation models also lend credence to the use of MRI-IPH as a cost-effective tool to identify patients with asymptomatic carotid stenosis likely to benefit from surgery.[53]

IPH Detection With MRI

For nearly 40 years, pathology studies on large-artery atherosclerosis have linked IPH to stroke etiology.[11,54–56] Only now, after 10 to 15 years of sequence development and histology validation, MRI has been perfected to image carotid IPH noninvasively.

T1-Weighted Sequences in IPH Detection

For some time, controversy existed concerning the specificity of T1-weighted (T1w) sequences in detecting carotid IPH. Most of the initial work using MRI on atherosclerotic plaque concentrated on T2-weighted (T2w) sequences. When T1w sequences were used, the primary aim was initially to detect plaque lipid. In addition, early studies were primarily performed on in vitro or animal specimens, limiting clinical application.[57–61] In the mid-1990s, Toussaint et al[62] used T2w sequences to discriminate plaque components, including lipid core, fibrous cap, calcification, normal media, adventitia, IPH, and thrombus. Other studies followed and used multiple MRI sequences (multicontrast MRI) to discriminate between complicated and uncomplicated plaques.[63,64]

In the early 2000s, T1w sequences were found to also detect IPH. In 2001, Yuan et al[65] found that both IPH and lipid/necrosis were T1 hyperintense. Later, in 2003, Murphy and Moody demonstrated that a T1w MRI sequence could identify complex plaque (AHA type VI) using the magnetization-prepared rapid acquisition gradient echo (MPRAGE) sequence.[13,43] Since then, these heavily T1w MRI sequences have been shown to have unparalleled sensitivity and specificity in detecting IPH when compared with other imaging techniques, including ultrasound, computed tomographic angiography, and digital subtraction angiography.[6]

A variety of T1w sequences can be used to detect carotid IPH (Table 1). These include 3-dimensional (3D) MPRAGE, 3D time-of-flight, and conventional T1w sequences. Of these sequences, MPRAGE has the highest specificity (97%) and sensitivity (80%) in the detection of carotid IPH compared with histology.[66] This was similar to results from earlier work in 2008 on another T1w sequence in which 97 images were compared with histology and demonstrated high accuracy, specificity, and sensitivity (87%-90%, 80%-88%, and 94%-100%, respectively).[67] More recently, the MPRAGE sequence was used to detect IPH and found to also correlate with large necrotic cores.[42] To determine which of these was being detected, another study found that MPRAGE-positive area correlated with IPH but not lipid or necrotic core (LNC) on a slice-by-slice comparison with histology slides.[68]

The reason for the high accuracy of MPRAGE is that various plaque components with a relatively long T1, such as fibrous tissue and the lipid-rich necrotic core, are also suppressed owing to the inversion-recovery preparation and fat saturation. This results in the MPRAGE sequence having the highest tissue contrast between IPH and background structures. Because of this and the multiple prior studies above demonstrating histologic validation, our group and others have adopted the MPRAGE as the standard method to diagnose carotid IPH.

MPRAGE Detection of Carotid IPH

Plaque is considered "MPRAGE positive" if it exceeds a 2-fold signal threshold over adjacent sternocleidomastoid muscle, as previously described.[68] Using the carotid MPRAGE sequence in patients prior to carotid surgery, we have found a very high (>90%) accuracy, sensitivity, and specificity in detecting IPH versus LNC (Figure 1).[68]

Table 1. MRI-IPH detection sequence parameters.

SEQUENCE PARAMETERS	3D-MPRAGE[78]	3D-TOF	3D-T1W FSE (VARIABLE FLIP ANGLE)	3D-SNAP[80]
Orientation	Oblique-coronal	Axial	Oblique-coronal	Oblique-coronal
Blood flow suppression	Nonselective inversion	Saturation slab for venous flow	DIR, QIR, or DANTE	Nonselective inversion
Resolution, mm, for 3D isotropic	0.5-0.8	0.5-0.8	0.8-1.0	0.5-0.8
No. of slices	80	64	64	80
TR/TE, ms	10/2.55	20/3.4	800/22	10/4.8
TI or prep. time, ms	350 (TI)		600 (TI) or 150 (DANTE prep.)	500 (TI)
Cartesian or SOS	SOS	Cartesian	Cartesian	Cartesian
Scan time, min	3-5	3-5	5-7	5-7
FOV, mm	160 × 160	160 × 160	160 × 160	160 × 160
Fat saturation	Yes	No	Yes	Yes
Reconstruction	Ciné or static	MPR, MIP		Phase-sensitive inversion

Abbreviations: 3D-MPRAGE, 3-dimensional magnetization-prepared rapid acquisition gradient echo; 3D-SNAP, 3D simultaneous noncontrast angiography and IPH; 3D-T1w FSE, 3-dimensional T1-weighted fast spin echo; 3D-TOF, 3D time-of-flight; DANTE, delay alternating with nutation for tailored excitation; DIR, double inversion recovery; FOV, field of view; MIP, maximum intensity projection; MPR, multiplanar reconstruction; QIR, quadruple inversion recovery; SOS, stack of stars; TI, inversion time; TR/TE, repetition time/echo time.

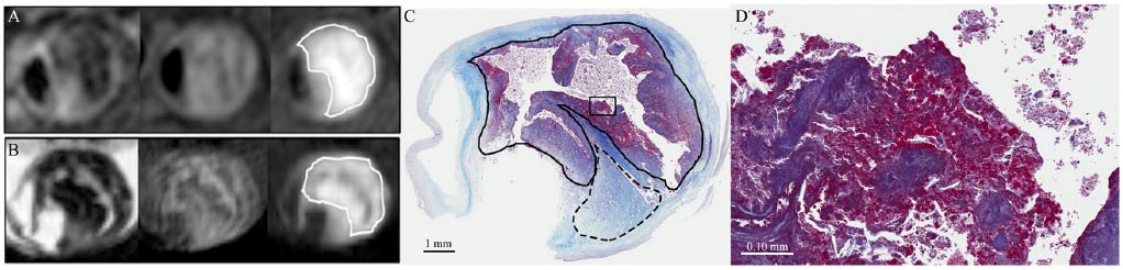

Figure 1. Intraplaque hemorrhage (IPH) detection and histology: (A) in vivo and (B) ex vivo 3-T magnetic resonance images of carotid plaque with T2-weighted, T1-weighted, and magnetization-prepared rapid acquisition gradient echo (MPRAGE) sequences from left to right. MPRAGE-positive plaque is outlined with a solid line, as defined using a 2-fold threshold compared with adjacent muscle. IPH and lipid/necrotic core were defined on histology with trichrome stain with (C) 1× and (D) 20× images. MPRAGE (+) signal corresponded to areas of IPH (solid line) as opposed to lipid/necrosis (dashed line). Hematoxylin-eosin and phosphotungstic acid hematoxylin stains were also used to confirm the presence of recent hemorrhage.

Specialized Versus Standard Neck Coils

With recent advances, carotid MRI is becoming a more useful tool in standard clinical practice. To fully transition to the clinic, high-sensitivity MRI coils must integrate well with the clinical environment and the variety of neck shapes and sizes. In many carotid imaging research studies, specialized neck coils are used to obtain images with high signal-to-noise ratio (SNR).[69–72] Early custom-made carotid coils consisted of bilateral dual-element phased array coils.[70,72] Initial results with specialized coils suggested that there was no significant advantage over standard clinical coils in the detection of IPH,[68] but this result may be more of an indication of the difficulty encountered using this type of specialized coils. Because prior coils typically required sponges and straps to position them on the patient's neck, it was difficult to position them without differences in pressure against the neck, and as a result, changes in normal neck configuration and blood flow can easily occur. In addition to the difficulty in positioning these coils, it was often required to reposition the coils to place them directly over the carotid bifurcation. These difficulties combined with the need to remove commercial coils from the patient's table before use and the extra time required to change out the coils and position them correctly on the patient have all but eliminated their use in the clinical setting.

Recently, we have designed coils as a single coil former that is designed to integrate with commercial coils.[73] Consequently, these coils are easy to position on a patient's neck with uniform pressure and without changes in neck

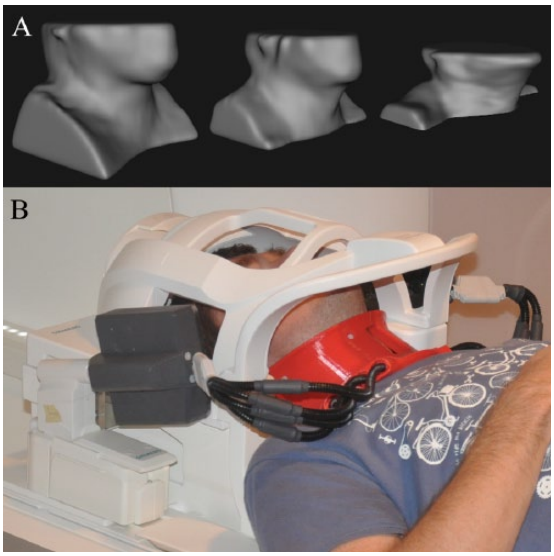

Figure 2. Neck-shape–specific coils. (A) Standard neck coils with a large all-encompassing anterior neck coil are made to accommodate all patient shapes and sizes at the expense of poor signal-to-noise ratio (SNR). (B) The standard magnetic resonance imaging head/neck coil can be fitted with a 7-channel neck-shape–specific coil that fits close to the surface of the neck. This provides significantly higher SNR than the commercial coil alone.

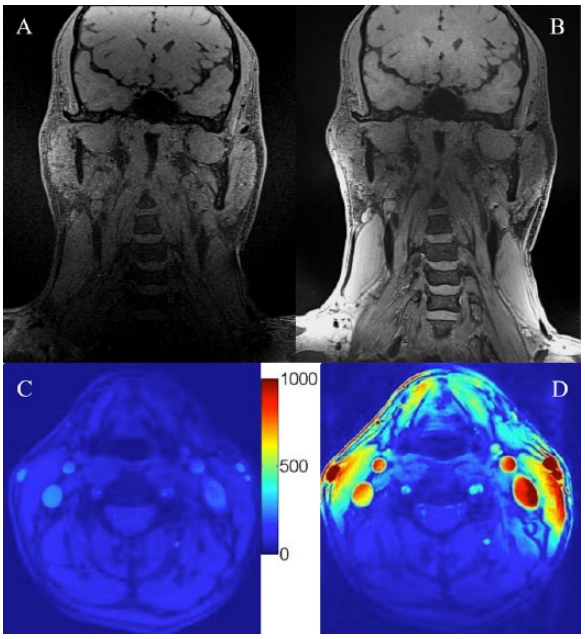

Figure 3. Full head/neck images with high signal-to-noise ratio (SNR) carotid coils: three-dimensional (3D) ciné-Retrospective Ordering and Compressed Sensing (ciné-ROCS), delay alternating with nutation for tailored excitation with fast low-angle shot (DASH) coronal images acquired with the standard magnetic resonance imaging (MRI) head/neck coil (A) without or (B) with the addition of 7-channel coils on the same volunteer. Imaging parameters for the 3D ciné-ROCS DASH image: isotropic voxel dimensions = 0.63 mm, repetition time/echo time = 2.5/8.0 ms, field of view = 240 × 240 mm, matrix size = 384 × 384 × 96, delay alternating with nutation for tailored excitation prep. = 150 ms, flip angle = 8.0°, and scan time = 8 minutes 20 seconds. SNR maps demonstrate 200- to 400-fold increased SNR comparing the standard MRI head/neck coil (C) without versus (D) with the 7-channel coils.

configuration and blood flow, and they do not require repositioning to place the coil over the bifurcation. Their integration with the commercial coils (Figure 2) eliminates the need to remove the commercial coils from the patient's table and allows the other coils to be used simultaneously in conjunction with the high-resolution neck coils for full head/neck imaging. Use of these coils combined with optimized pulse sequences also allows full coverage of the head and neck with high-resolution, efficient imaging of the craniocervical vasculature, making the technique easily adaptable to the clinical setting (Figure 3). These coils can give very high SNR, with gains of approximately 200% to 400% over standard clinical anterior neck coils, depending on carotid depth.

1.5 T Versus 3 T

For the MPRAGE sequence to transition from the research to clinical setting, it was important that intra- and interrater reliability remain high at 1.5 T compared with 3 T. In applying the sequence to a large clinical population, MPRAGE had very good inter- and intrarater reliability at 1.5 T, similar to 3 T. The prevalence-adjusted and bias-adjusted kappa values at 1.5 T remained as high at 3 T. These results argue that carotid IPH detection with MRI, previously isolated to 3 T research subjects, can be used clinically at 1.5 T.[68]

Surprisingly, image quality at 1.5 T was rated higher than 3 T by radiologists, even after controlling for potential confounders (body mass index, age, male sex, and MPRAGE-positive signal). This was secondary to slightly increased image artifacts at 3 T compared with 1.5 T images, a well-known limitation of high-field imaging.[74] Identifying and correcting the limitations of carotid MRI are extremely important as the MPRAGE sequence is increasingly added to the clinical workup of stroke and future clinical trials. As IPH detection changes from a binary diagnosis (present versus absent) to a volumetric measurement to monitor treatment effect and failure, accurate quantification of IPH volume is required. This requires neuroradiologists to be aware of potential artifacts and sequence modifications to obtain optimal SNR at 3 T.

MPRAGE Limitations

MPRAGE image quality can be degraded by a variety of factors. These include motion from respiration or cardiac pulsation, incomplete blood flow suppression, incomplete fat saturation, and decreased SNR.[68] The 3 T MRI has the advantage of increased SNR over 1.5 T and allows higher resolution imaging of small plaques. Still, 3 T imaging is not without disadvantages. Motion artifacts secondary to view-to-view phase errors result in signal amplitude variation and ghosting proportional to magnetic field strength. Fat saturation failure secondary to B0 inhomogeneity is a known complication of 3 T imaging, with susceptibility variations 2-fold higher than at 1.5 T. These artifacts can be decreased by improved field shimming and isocenter positioning of the carotid bifurcations.[75] Flow artifacts can also be more evident at 3 T compared with

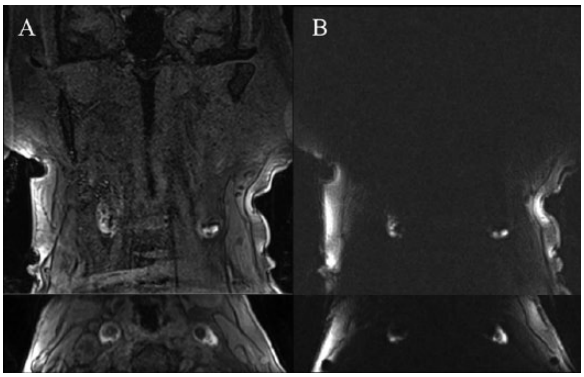

Figure 4. Optimized magnetic resonance imaging-intraplaque hemorrhage imaging with magnetization-prepared rapid acquisition gradient echo (MPRAGE): comparison of (A) standard Cartesian MPRAGE (top = coronal, bottom = axial reformat) with (B) an optimized stack of stars MPRAGE sequence (top = coronal, bottom = axial reformat) demonstrates complete suppression of flow artifact and background tissue signal. This patient has bilateral carotid intraplaque hemorrhage centered at the bifurcations. Both sequences were acquired in the same patient with neck-shape–specific coils.

1.5 T due to magnified effects of susceptibility-induced inhomogeneity.[68,75,76] In addition to the above limitations, IPH is also difficult to detect when present in small amounts or in the setting of heavy calcification.[66]

In an effort to improve interrater reliability, the MPRAGE sequence has been modified and alternative methods have been developed to overcome these potential limitations. Flow artifact and cardiac pulsation artifacts can be eliminated by applying cardiac gating and postprocessing to create a ciné-MPRAGE sequence.[77] Furthermore, the radial-based k-space trajectory stack of stars (SOS) MPRAGE results in more robust flow suppression, reduced motion sensitivity, and higher image quality compared with Cartesian MPRAGE while retaining high interrater reliability (Figure 4).[78] These sequences suppress all background tissue and flow-related signal and will enable automated IPH volume calculation.

Alternative methods can also separate flow artifact from high wall signal. The slab-selective phase-sensitive inversion-recovery technique was developed by combining a phase-sensitive reconstruction with a T1w sequence designed to achieve improved IPH imaging.[79] More recently, 3D Simultaneous Noncontrast Angiography and IPH (3D-SNAP) was developed to simultaneously detect lumen stenosis and IPH and was comparable with MPRAGE (kappa = 0.82).[80] However, the SNAP sequence is more motion limited in practice due to longer, approximate double imaging times compared with MPRAGE (Table 1). Multisequence methods such as multicontrast atherosclerosis characterization simultaneously obtain 3 different contrast weightings (hyper-T1w, T2w, and gray blood) in a 5-minute scan and can separately image IPH, lipid/necrosis, and calcification.[81,82] These novel methods may represent future alternatives or additions to MPRAGE imaging.

Other sequences have also been used to help age and characterize blood products in carotid IPH. The calculated water diffusion coefficients (apparent diffusion coefficient [ADC]) in different components within atherosclerotic plaques suggest that diffusion-weighted imaging (DWI) might also provide a tool for discriminating IPH and LNC from other plaque components.[83] Diffusion-weighted imaging evaluation of hemorrhage and calculation of the ADC in vitro reflect the stages of thrombus aging and organization.[84] Lower ADC values have also been associated with carotid IPH and may provide additional information on hemorrhage age, plaque vulnerability, and future stroke risk.[85] Future studies will be needed to determine that IPH ADC values add significant discrimination to stroke risk.

Additional Markers of MRI-Detected IPH

Much like duplex carotid ultrasound, peak systolic velocity can be used as a surrogate marker for percent diameter stenosis, and other imaging findings hint to the likelihood of carotid IPH. Research has found that IPH likelihood increases with degree of carotid stenosis.[86] Intraplaque hemorrhage also positively correlates with plaque volume and thickness.[87] Computed tomographic angiography–detected ulceration can also be used to predict IPH.[88] In addition to these imaging markers, IPH has been found at higher prevalence in men and in higher age groups.[89]

With these findings in mind, predictive models of IPH have been developed. Maximum plaque thickness, millimeter stenosis, ulceration, age, and male sex can predict carotid IPH with a high discriminatory power.[90] The finding that plaque ulceration is strongly predictive of IPH may suggest that IPH may predispose to endothelial dysfunction, erosion, and eventual ulceration through proinflammatory effects of iron on reactive oxygen species formation.[91] The association of thickness with IPH suggests that larger plaques are inherently more unstable and prone to hemorrhage, potentially due to a larger lipid-rich core and/or a higher number or more permeable plaque neovessels. Results from studies with dynamic contrast-enhanced magnetic resonance imaging suggest that microvascular permeability predisposes to IPH.[92,93]

In addition, stenosis is a significant indicator of IPH, which may be related to impaired flow dynamics and oscillatory shear stress given that IPH develops in areas of stenosis and low wall shear stress.[94] Low mean shear stress and in particular oscillatory shear stress lead to altered endothelial cell mechanotransduction and endothelial reactive oxygen species formation in cell culture models.[95–98] Oscillatory shear stress at branch points and downstream of stenosis could stimulate IPH through local inflammation and microvessel leakage. Age is also associated with IPH, and this may be related to increased levels of oxidative stress, DNA damage, mitochondrial dysfunction, and altered balance of cell proliferation and apoptosis.[99] The increased likelihood of IPH in men may be related to the protective effect of estrogen in women or sex differences in platelet activation or endothelial cell function.[100,101]

These studies may provide clues to the pathogenesis of IPH. Animal models also indicate that IPH can be stimulated by angiotensin II administration.[102] In a human study, however, IPH was not associated with angiotensin II levels, but instead with low vitamin D.[103] Vitamin D is a known negative regulator of the angiotensin system and may have local effects on the vessel wall.[104] Although some have postulated that hypertension induces neovessel rupture and IPH, only a few studies have found a link between hypertension and IPH. Confounding by antihypertensive use may explain this. When controlling for antihypertensives, studies have found no association with elevated blood pressure.[90] Recently, carotid IPH was independently associated instead with low diastolic blood pressure and was not attributed to medication differences.[105] Furthermore, studies have found an association between carotid IPH and antiplatelet use.[105,106] These and the above associative studies represent steps toward understanding the pathophysiology and will lead to future clinical trials aimed at decreasing carotid IPH and future stroke risk.

Conclusions

In summary, accurate detection of carotid IPH is accomplished using advanced, heavily T1w techniques, including the MPRAGE sequence. Intraplaque hemorrhage has been established as a primary determinant of carotid plaque instability. Magnetic resonance imaging detection of IPH is possible on all vendor platforms with standard pulse sequences and can be accomplished at both 3 and 1.5 T. It is important to be aware of the potential MRI-IPH artifacts, including motion degradation, fat saturation failure, and incomplete flow suppression. To counteract these potential artifacts, one should consider a modified sequence, such as the SOS-MPRAGE technique. Nevertheless, using the MPRAGE sequence, IPH determination has been validated with histology and has high intra- and interrater reliability at both 1.5 and 3 T field strengths. Advances in ciné imaging, motion-insensitive MPRAGE, and form-fitting high SNR coils allow quantification of IPH volume at 3 T. The MRI-IPH imaging will be required for randomized controlled trials to determine the potential benefit of novel medications, surgical intervention, or stenting. Now that IPH can be detected noninvasively, our goal is to reduce primary and secondary stroke risk in this vulnerable population.

Author Contributions

JSM wrote the first draft of the manuscript. JSM, SEK, JM, JRH, AS, AHD, GST, and DLP contributed to the writing of the manuscript, agree with manuscript results and conclusions, jointly developed the structure and arguments for the paper, made critical revisions, and approved the final version. All authors reviewed and approved the final manuscript.

Disclosures and Ethics

As a requirement of publication, author(s) have provided to the publisher signed confirmation of compliance with legal and ethical obligations including, but not limited to, the following: authorship and contributorship, conflicts of interest, privacy and confidentiality, and (where applicable) protection of human and animal research subjects. The authors have read and confirmed their agreement with the ICMJE authorship and conflict of interest criteria. The authors have also confirmed that this article is unique and not under consideration or published in any other publication, and that they have permission from rights holders to reproduce any copyrighted material. Any disclosures are made in this section. The external blind peer reviewers report no conflicts of interest.

REFERENCES

1. Mozaffarian D, Benjamin EJ, Go AS, et al. Heart disease and stroke statistics-2015 update: a report from the American Heart Association. *Circulation*. 2015;131:e29–e322.
2. Go AS, Mozaffarian D, Roger VL, et al. Heart disease and stroke statistics—2013 update: a report from the American Heart Association. *Circulation*. 2013;127:e6–e245.
3. Clinical alert: benefit of carotid endarterectomy for patients with high-grade stenosis of the internal carotid artery. National Institute of Neurological Disorders and Stroke Stroke and Trauma Division. North American Symptomatic Carotid Endarterectomy Trial (NASCET) investigators. *Stroke*. 1991;22:816–817.
4. Endarterectomy for asymptomatic carotid artery stenosis. Executive Committee for the Asymptomatic Carotid Atherosclerosis Study. *JAMA*. 1995;273:1421–1428.
5. Altaf N, Beech A, Goode SD, et al. Carotid intraplaque hemorrhage detected by magnetic resonance imaging predicts embolization during carotid endarterectomy. *J Vasc Surg*. 2007;46:31–36.
6. Chu B, Kampschulte A, Ferguson MS, et al. Hemorrhage in the atherosclerotic carotid plaque: a high-resolution MRI study. *Stroke*. 2004;35:1079–1084.
7. Fryer JA, Myers PC, Appleberg M. Carotid intraplaque hemorrhage: the significance of neovascularity. *J Vasc Surg*. 1987;6:341–349.
8. Gortler M, Goldmann A, Mohr W, Widder B. Tissue characterisation of atherosclerotic carotid plaques by MRI. *Neuroradiology*. 1995;37:631–635.
9. Li ZY, Howarth SP, Tang T, et al. Structural analysis and magnetic resonance imaging predict plaque vulnerability: a study comparing symptomatic and asymptomatic individuals. *J Vasc Surg*. 2007;45:768–775.
10. Lovett JK, Gallagher PJ, Hands LJ, Walton J, Rothwell PM. Histological correlates of carotid plaque surface morphology on lumen contrast imaging. *Circulation*. 2004;110:2190–2197.
11. Lusby RJ, Ferrell LD, Ehrenfeld WK, Stoney RJ, Wylie EJ. Carotid plaque hemorrhage. Its role in production of cerebral ischemia. *Arch Surg*. 1982;117:1479–1488.
12. Mofidi R, Crotty TB, McCarthy P, Sheehan SJ, Mehigan D, Keaveny TV. Association between plaque instability, angiogenesis and symptomatic carotid occlusive disease. *Br J Surg*. 2001;88:945–950.
13. Moody AR, Murphy RE, Morgan PS, et al. Characterization of complicated carotid plaque with magnetic resonance direct thrombus imaging in patients with cerebral ischemia. *Circulation*. 2003;107:3047–3052.
14. Ouhlous M, Flach HZ, de Weert TT, et al. Carotid plaque composition and cerebral infarction: MR imaging study. *AJNR Am J Neuroradiol*. 2005;26:1044–1049.
15. Raman SV, Winner MW 3rd, Tran T, et al. In vivo atherosclerotic plaque characterization using magnetic susceptibility distinguishes symptom-producing plaques. *JACC Cardiovasc Imaging*. 2008;1:49–57.
16. Saam T, Hatsukami TS, Takaya N, et al. The vulnerable, or high-risk, atherosclerotic plaque: noninvasive MR imaging for characterization and assessment. *Radiology*. 2007;244:64–77.
17. Sharma R. MR imaging in carotid artery atherosclerosis plaque characterization. *Magn Reson Med Sci*. 2002;1:217–232.
18. Singh N, Moody AR, Gladstone DJ, et al. Moderate carotid artery stenosis: MR imaging-depicted intraplaque hemorrhage predicts risk of cerebrovascular ischemic events in asymptomatic men. *Radiology*. 2009;252:502–508.
19. Spagnoli LG, Mauriello A, Sangiorgi G, et al. Extracranial thrombotically active carotid plaque as a risk factor for ischemic stroke. *JAMA*. 2004;292:1845–1852.
20. Virmani R, Ladich ER, Burke AP, Kolodgie FD. Histopathology of carotid atherosclerotic disease. *Neurosurgery*. 2006;59:S219–S227; discussion S213-S213.

21. Wallis de Vries BM, van Dam GM, Tio RA, Hillebrands JL, Slart RH, Zeebregts CJ. Current imaging modalities to visualize vulnerability within the atherosclerotic carotid plaque. *J Vasc Surg*. 2008;48:1620–1629.
22. Lloyd-Jones DM, Hong Y, Labarthe D, et al. Defining and setting national goals for cardiovascular health promotion and disease reduction: the American Heart Association's strategic impact goal through 2020 and beyond. *Circulation*. 2010;121:586–613.
23. Stary HC, Chandler AB, Dinsmore RE, et al. A definition of advanced types of atherosclerotic lesions and a histological classification of atherosclerosis. A report from the Committee on Vascular Lesions of the Council on Arteriosclerosis, American Heart Association. *Circulation*. 1995;92:1355–1374.
24. Schoenhagen P, Ziada KM, Vince DG, Nissen SE, Tuzcu EM. Arterial remodeling and coronary artery disease: the concept of "dilated" versus "obstructive" coronary atherosclerosis. *J Am Coll Cardiol*. 2001;38:297–306.
25. Norris JW, Zhu CZ. Stroke risk and critical carotid stenosis. *J Neurol Neurosurg Psychiatry*. 1990;53:235–237.
26. Morgenstern LB, Fox AJ, Sharpe BL, Eliasziw M, Barnett HJ, Grotta JC. The risks and benefits of carotid endarterectomy in patients with near occlusion of the carotid artery. North American Symptomatic Carotid Endarterectomy Trial (NASCET) Group. *Neurology*. 1997;48:911–915.
27. Fox AJ, Eliasziw M, Rothwell PM, Schmidt MH, Warlow CP, Barnett HJ. Identification, prognosis, and management of patients with carotid artery near occlusion. *AJNR Am J Neuroradiol*. 2005:26:2086–2094.
28. Virmani R, Kolodgie FD, Burke AP, et al. Atherosclerotic plaque progression and vulnerability to rupture: angiogenesis as a source of intraplaque hemorrhage. *Arterioscler Thromb Vasc Biol*. 2005:25:2054–2061.
29. Kumamoto M, Nakashima Y, Sueishi K. Intimal neovascularization in human coronary atherosclerosis: its origin and pathophysiological significance. *Hum Pathol*. 1995;26:450–456.
30. Fleiner M, Kummer M, Mirlacher M, et al. Arterial neovascularization and inflammation in vulnerable patients: early and late signs of symptomatic atherosclerosis. *Circulation*. 2004;110:2843–2850.
31. Lappalainen H, Laine P, Pentikainen MO, Sajantila A, Kovanen PT. Mast cells in neovascularized human coronary plaques store and secrete basic fibroblast growth factor, a potent angiogenic mediator. *Arterioscler Thromb Vasc Biol*. 2004:24:1880–1885.
32. Sluimer JC, Kolodgie FD, Bijnens AP, et al. Thin-walled microvessels in human coronary atherosclerotic plaques show incomplete endothelial junctions relevance of compromised structural integrity for intraplaque microvascular leakage. *J Am Coll Cardiol*. 2009;53:1517–1527.
33. Sun J, Underhill HR, Hippe DS, Xue Y, Yuan C, Hatsukami TS. Sustained acceleration in carotid atherosclerotic plaque progression with intraplaque hemorrhage: a long-term time course study. *JACC Cardiovasc Imaging*. 2012;5:798–804.
34. Hao H, Iihara K, Ishibashi-Ueda H, Saito F, Hirota S. Correlation of thin fibrous cap possessing adipophilin-positive macrophages and intraplaque hemorrhage with high clinical risk for carotid endarterectomy. *J Neurosurg*. 2011;114:1080–1087.
35. Watanabe Y, Nagayama M, Sakata A, et al. Evaluation of fibrous cap rupture of atherosclerotic carotid plaque with thin-slice source images of time-of-flight MR angiography. *Ann Vasc Dis*. 2014;7:127–133.
36. Daemen MJ, Ferguson MS, Gijsen FJ, et al. Carotid plaque fissure: an underestimated source of intraplaque hemorrhage. *Atherosclerosis*. 2016;254:102–108.
37. Altaf N, MacSweeney ST, Gladman J, Auer DP. Carotid intraplaque hemorrhage predicts recurrent symptoms in patients with high-grade carotid stenosis. *Stroke*. 2007;38:1633–1635.
38. Moore WS, Hall AD. Ulcerated atheroma of the carotid artery. A cause of transient cerebral ischemia. *Am J Surg*. 1968;116:237–242.
39. Moore WS, Hall AD. Importance of emboli from carotid bifurcation in pathogenesis of cerebral ischemic attacks. *Arch Surg*. 1970;101:708–711.
40. Parmar JP, Rogers WJ, Mugler JP 3rd, et al. Magnetic resonance imaging of carotid atherosclerotic plaque in clinically suspected acute transient ischemic attack and acute ischemic stroke. *Circulation*. 2010;122:2031–2038.
41. Saam T, Cai J, Ma L, et al. Comparison of symptomatic and asymptomatic atherosclerotic carotid plaque features with in vivo MR imaging. *Radiology*. 2006;240:464–472.
42. Hishikawa T, Iihara K, Yamada N, Ishibashi-Ueda H, Miyamoto S. Assessment of necrotic core with intraplaque hemorrhage in atherosclerotic carotid artery plaque by MR imaging with 3D gradient-echo sequence in patients with high-grade stenosis. *J Neurosurg*. 2010;113:890–896.
43. Murphy RE, Moody AR, Morgan PS, et al. Prevalence of complicated carotid atheroma as detected by magnetic resonance direct thrombus imaging in patients with suspected carotid artery stenosis and previous acute cerebral ischemia. *Circulation*. 2003;107:3053–3058.
44. Rao DS, Goldin JG, Fishbein MC. Determinants of plaque instability in atherosclerotic vascular disease. *Cardiovasc Pathol*. 2005;14:285–293.
45. Takaya N, Yuan C, Chu B, et al. Presence of intraplaque hemorrhage stimulates progression of carotid atherosclerotic plaques: a high-resolution magnetic resonance imaging study. *Circulation*. 2005;111:2768–2775.
46. Yamada N, Higashi M, Otsubo R, et al. Association between signal hyperintensity on T1-weighted MR imaging of carotid plaques and ipsilateral ischemic events. *AJNR Am J Neuroradiol*. 2007;28:287–292.
47. Takaya N, Yuan C, Chu B, et al. Association between carotid plaque characteristics and subsequent ischemic cerebrovascular events: a prospective assessment with MRI—initial results. *Stroke*. 2006;37:818–823.
48. Gupta A, Baradaran H, Schweitzer AD, et al. Carotid plaque MRI and stroke risk: a systematic review and meta-analysis. *Stroke*. 2013;44:3071–3077.
49. Hosseini AA, Kandiyil N, Macsweeney ST, Altaf N, Auer DP. Carotid plaque hemorrhage on magnetic resonance imaging strongly predicts recurrent ischemia and stroke. *Ann Neurol*. 2013;73:774–784.
50. Saam T, Hetterich H, Hoffmann V, et al. Meta-analysis and systematic review of the predictive value of carotid plaque hemorrhage on cerebrovascular events by magnetic resonance imaging. *J Am Coll Cardiol*. 2013;62:1081–1091.
51. McNally JS, Kim SE, Yoon HC, et al. Carotid magnetization-prepared rapid acquisition with gradient-echo signal is associated with acute territorial cerebral ischemic events detected by diffusion-weighted MRI. *Circ Cardiovasc Imaging*. 2012;5:376–382.
52. McNally JS, McLaughlin MS, Hinckley PJ, et al. Intraluminal thrombus, intraplaque hemorrhage, plaque thickness, and current smoking optimally predict carotid stroke. *Stroke*. 2015;46:84–90.
53. Gupta A, Mushlin AI, Kamel H, Navi BB, Pandya A. Cost-effectiveness of carotid plaque MR imaging as a stroke risk stratification tool in asymptomatic carotid artery stenosis. *Radiology*. 2015;277:763–772.
54. Burke AP, Kolodgie FD, Farb A, et al. Healed plaque ruptures and sudden coronary death: evidence that subclinical rupture has a role in plaque progression. *Circulation*. 2001;103:934–940.
55. Davies AH, Hayward JK, Currie I, et al. Risk prediction of outcome following carotid endarterectomy. *Cardiovasc Surg*. 1996;4:338–339.
56. Sadoshima S, Fukushima T, Tanaka K. Cerebral artery thrombosis and intramural hemorrhage. *Stroke*. 1979;10:411–414.
57. Herfkens RJ, Higgins CB, Hricak H, et al. Nuclear magnetic resonance imaging of atherosclerotic disease. *Radiology*. 1983;148:161–166.
58. Skinner MP, Yuan C, Mitsumori L, et al. Serial magnetic resonance imaging of experimental atherosclerosis detects lesion fine structure, progression and complications in vivo. *Nat Med*. 1995;1:69–73.
59. Gold GE, Pauly JM, Glover GH, Moretto JC, Macovski A, Herfkens RJ. Characterization of atherosclerosis with a 1.5-T imaging system. *J Magn Reson Imaging*. 1993;3:399–407.
60. Toussaint JF, Southern JF, Fuster V, Kantor HL. T2-weighted contrast for NMR characterization of human atherosclerosis. *Arterioscler Thromb Vasc Biol*. 1995;15:1533–1542.
61. Maynor CH, Charles HC, Herfkens RJ, Suddarth SA, Johnson GA. Chemical shift imaging of atherosclerosis at 7.0 Tesla. *Invest Radiol*. 1989;24:52–60.
62. Toussaint JF, LaMuraglia GM, Southern JF, Fuster V, Kantor HL. Magnetic resonance images lipid, fibrous, calcified, hemorrhagic, and thrombotic components of human atherosclerosis in vivo. *Circulation*. 1996;94:932–938.
63. Yuan C, Zhang SX, Polissar NL, et al. Identification of fibrous cap rupture with magnetic resonance imaging is highly associated with recent transient ischemic attack or stroke. *Circulation*. 2002;105:181–185.
64. Cai JM, Hatsukami TS, Ferguson MS, Small R, Polissar NL, Yuan C. Classification of human carotid atherosclerotic lesions with in vivo multicontrast magnetic resonance imaging. *Circulation*. 2002;106:1368–1373.
65. Yuan C, Mitsumori LM, Ferguson MS, et al. In vivo accuracy of multispectral magnetic resonance imaging for identifying lipid-rich necrotic cores and intraplaque hemorrhage in advanced human carotid plaques. *Circulation*. 2001;104:2051–2056.
66. Ota H, Yarnykh VL, Ferguson MS, et al. Carotid intraplaque hemorrhage imaging at 3.0-T MR imaging: comparison of the diagnostic performance of three T1-weighted sequences. *Radiology*. 2010;254:551–563.
67. Bitar R, Moody AR, Leung G, et al. In vivo 3D high-spatial-resolution MR imaging of intraplaque hemorrhage. *Radiology*. 2008;249:259–267.
68. McNally JS, Yoon HC, Kim SE, et al. Carotid MRI detection of intraplaque hemorrhage at 3T and 1.5T. *J Neuroimaging*. 2015;25:390–396.
69. Balu N, Yarnykh VL, Scholnick J, Chu B, Yuan C, Hayes C. Improvements in carotid plaque imaging using a new eight-element phased array coil at 3T. *J Magn Reson Imaging*. 2009;30:1209–1214.
70. Hayes CE, Mathis CM, Yuan C. Surface coil phased arrays for high-resolution imaging of the carotid arteries. *J Magn Reson Imaging*. 1996;6:109–112.
71. Tate Q, Kim SE, Treiman G, Parker DL, Hadley JR. Increased vessel depiction of the carotid bifurcation with a specialized 16-channel phased array coil at 3T. *Magn Reson Med*. 2013;69:1486–1493.

72. Hadley JR, Roberts JA, Goodrich KC, Buswell HR, Parker DL. Relative RF coil performance in carotid imaging. *Magn Reson Imaging*. 2005;23:629–639.
73. Beck MJ, Parker DL, Bolster BD Jr, et al. Interchangeable neck shape-specific coils for a clinically realizable anterior neck phased array system. *Magn Reson Med*. 2017; Epub ahead of print.
74. Chavhan GB, Babyn PS, Singh M, Vidarsson L, Shroff M. MR imaging at 3.0 T in children: technical differences, safety issues, and initial experience. *Radiographics*. 2009;29:1451–1466.
75. Bernstein MA, Huston J 3rd, Ward HA. Imaging artifacts at 3.0T. *J Magn Reson Imaging*. 2006;24:735–746.
76. Drangova M, Pelc NJ. Artifacts and signal loss due to flow in the presence of B(o) inhomogeneity. *Magn Reson Med*. 1996;35:126–130.
77. Mendes J, Parker DL, Kim SE, Treiman GS. Reduced blood flow artifact in intraplaque hemorrhage imaging using CineMPRAGE. *Magn Reson Med*. 2013;69:1276–1284.
78. Kim SE, Roberts JA, Eisenmenger LB, et al. Motion-insensitive carotid intraplaque hemorrhage imaging using 3D inversion recovery preparation stack of stars (IR-prep SOS) technique. *J Magn Reson Imaging*. 2017;45: 410–417.
79. Wang J, Ferguson MS, Balu N, Yuan C, Hatsukami TS, Bornert P. Improved carotid intraplaque hemorrhage imaging using a slab-selective phase-sensitive inversion-recovery (SPI) sequence. *Magn Reson Med*. 2010;64:1332–1340.
80. Wang J, Bornert P, Zhao H, et al. Simultaneous noncontrast angiography and intraplaque hemorrhage (SNAP) imaging for carotid atherosclerotic disease evaluation. *Magn Reson Med*. 2013;69:337–345.
81. Dai Y, Lv P, Lin J, et al. Comparison study between multicontrast atherosclerosis characterization (MATCH) and conventional multicontrast MRI of carotid plaque with histology validation [published online ahead of print August 24, 2016]. *J Magn Reson Imaging*. doi:10.1002/jmri.25444.
82. Fan Z, Yu W, Xie Y, et al. Multi-contrast atherosclerosis characterization (MATCH) of carotid plaque with a single 5-min scan: technical development and clinical feasibility. *J Cardiovasc Magn Reson*. 2014;16:53.
83. Clarke SE, Hammond RR, Mitchell JR, Rutt BK. Quantitative assessment of carotid plaque composition using multicontrast MRI and registered histology. *Magn Reson Med*. 2003;50:1199–1208.
84. Toussaint JF, Southern JF, Fuster V, Kantor HL. Water diffusion properties of human atherosclerosis and thrombosis measured by pulse field gradient nuclear magnetic resonance. *Arterioscler Thromb Vasc Biol*. 1997;17:542–546.
85. Yao B, Yang L, Wang G, et al. Diffusion measurement of intraplaque hemorrhage and intramural hematoma using diffusion weighted MRI at 3T in cervical artery. *Eur Radiol*. 2016;26:3737–3743.
86. Sun J, Song Y, Chen H, et al. Adventitial perfusion and intraplaque hemorrhage: a dynamic contrast-enhanced MRI study in the carotid artery. *Stroke*. 2013;44:1031–1036.
87. Zhao X, Underhill HR, Zhao Q, et al. Discriminating carotid atherosclerotic lesion severity by luminal stenosis and plaque burden: a comparison utilizing high-resolution magnetic resonance imaging at 3.0 Tesla. *Stroke*. 2011;42: 347–353.
88. U-King-Im JM, Fox AJ, Aviv RI, et al. Characterization of carotid plaque hemorrhage: a CT angiography and MR intraplaque hemorrhage study. *Stroke*. 2010;41:1623–1629.
89. Zhao XQ, Hatsukami TS, Hippe DS, et al. Clinical factors associated with high-risk carotid plaque features as assessed by magnetic resonance imaging in patients with established vascular disease (from the AIM-HIGH Study). *Am J Cardiol*. 2014;114:1412–1419.
90. McLaughlin A, Hinckley PJ, Treiman SM, et al. Optimal prediction of carotid intraplaque hemorrhage using clinical and lumen imaging markers. *AJNR Am J Neuroradiol*. 2015;36:2360–2366.
91. Buttari B, Profumo E, Businaro R, et al. Oxidized haemoglobin-driven endothelial dysfunction and immune cell activation: novel therapeutic targets for atherosclerosis. *Curr Med Chem*. 2013;20:4806–4814.
92. Kerwin WS, O'Brien KD, Ferguson MS, Polissar N, Hatsukami TS, Yuan C. Inflammation in carotid atherosclerotic plaque: a dynamic contrast-enhanced MR imaging study. *Radiology*. 2006;241:459–468.
93. Mendes J, Parker DL, McNally S, DiBella E, Bolster BD Jr., Treiman GS. Three-dimensional dynamic contrast enhanced imaging of the carotid artery with direct arterial input function measurement. *Magn Reson Med*. 2014;72: 816–822.
94. Cheng C, Tempel D, van Haperen R, et al. Atherosclerotic lesion size and vulnerability are determined by patterns of fluid shear stress. *Circulation*. 2006;113:2744–2753.
95. McNally JS, Davis ME, Giddens DP, et al. Role of xanthine oxidoreductase and NAD(P)H oxidase in endothelial superoxide production in response to oscillatory shear stress. *Am J Physiol Heart Circ Physiol*. 2003;285: H2290–H2297.
96. Davies PF, Polacek DC, Shi C, Helmke BP. The convergence of haemodynamics, genomics, and endothelial structure in studies of the focal origin of atherosclerosis. *Biorheology*. 2002;39:299–306.
97. Pedersen EM, Oyre S, Agerbaek M, et al. Distribution of early atherosclerotic lesions in the human abdominal aorta correlates with wall shear stresses measured in vivo. *Eur J Vasc Endovasc Surg*. 1999;18:328–333.
98. Wentzel JJ, Kloet J, Andhyiswara I, et al. Shear-stress and wall-stress regulation of vascular remodeling after balloon angioplasty: effect of matrix metalloproteinase inhibition. *Circulation*. 2001;104:91–96.
99. Sobenin IA, Zhelankin AV, Sinyov VV, Bobryshev YV, Orekhov AN. Mitochondrial aging: focus on mitochondrial DNA damage in atherosclerosis—a mini-review. *Gerontology*. 2014;61:343–349.
100. Akishita M, Yu J. Hormonal effects on blood vessels. *Hypertens Res*. 2012;35:363–369.
101. Roy-O'Reilly M, McCullough LD. Sex differences in stroke: the contribution of coagulation. *Exp Neurol*. 2014;259:16–27.
102. da Cunha V, Martin-McNulty B, Vincelette J, et al. Angiotensin II induces histomorphologic features of unstable plaque in a murine model of accelerated atherosclerosis. *J Vasc Surg*. 2006;44:364–371.
103. McNally JS, Burton TM, Aldred BW, et al. Vitamin D and vulnerable carotid plaque [published online ahead of print June 16, 2016]. *AJNR Am J Neuroradiol*. doi:10.3174/ajnr.A4849.
104. Forman JP, Williams JS, Fisher ND. Plasma 25-hydroxyvitamin D and regulation of the renin-angiotensin system in humans. *Hypertension*. 2010;55: 1283–1288.
105. Sun J, Canton G, Balu N, et al. Blood pressure is a major modifiable risk factor implicated in pathogenesis of intraplaque hemorrhage: an in vivo magnetic resonance imaging study. *Arterioscler Thromb Vasc Biol*. 2016;36:743–749.
106. Liem MI, Schreuder FH, van Dijk AC, et al. Use of antiplatelet agents is associated with intraplaque hemorrhage on carotid magnetic resonance imaging: the plaque at risk study. *Stroke*. 2015;46:3411–3415.